Gas-Phase Decomposition Reactions of Tris(dimethylamino)phosphine, -arsine, and -stibine Reagents

Sateria Salim,[†] Chee Kiang Lim,[‡] and Klavs F. Jensen*,[‡]

Departments of Chemistry and Chemical Engineering, Massachusetts Institute of Technology, Cambridge, Massachusetts 02139

Received September 1, 1994. Revised Manuscript Received January 11, 1995[⊗]

Gas-phase pyrolysis of tris(dimethylamino)phosphine (DMAP), tris(dimethylamino)arsine (DMAAs), and tris(dimethylamino)stibine (DMASb) relevant to organometallic chemical vapor deposition (OMCVD) has been investigated using fiber-optic-based Fourier transform infrared spectroscopy and molecular beam mass spectrometry. Gas-phase decomposition studies in H_2, D_2, and He reveal that the primary pathway is homolysis of the E–N (E = P, As, Sb) bond, leading to the formation of dimethylaminyl radicals. The pyrolysis proceeds according to a first-order process, with activation energies of 50.6, 44.0, and 41.1 kcal/mol for DMAP, DMAAs, and DMASb, respectively. Subsequent interactions of dimethylaminyl radicals result in the formation of the stable products: methylmethyleneimine, dimethylamine, methyleneimine, and methane. At temperatures higher than 550 °C, the dimethylaminyl radical decomposes with the generation of ammonia and methane as primary products in hydrogen.

Introduction

Significant efforts have been expended in the development of organometallic sources for replacement of arsine and phosphine in organometallic chemical vapor deposition (OMCVD) of III–V compound semiconductors for optoelectronic applications.[1,2] Safety concerns over the use of high-pressure, toxic hydride sources have motivated research on low-vapor-pressure liquid organometallic sources, such as mono-*tert*-butylarsine and -phosphine. There has also been interest in organometallic antimony sources for low-temperature growth of Sb-containing compound semiconductors, which often are highly temperature sensitive.[2] The wide-range organometallic reagents explored in OMCVD growth and thermal decomposition studies have been reviewed by Stringfellow[2] and, more recently, by Jones.[3] Briefly, two primary categories of reagents have been investigated: trialkyl sources (e.g., trimethylarsenic, triethylarsenic, trimethylphosphorus, triisopropylantimony) and alkyl hydride sources (e.g., mono-*tert*-butylarsine, monophenylarsine, and mono-*tert*-butylphosphine).

Tris(dimethylamino)arsine (DMAAs), tris(dimethylamino)phosphine (DMAP), and tris(dimethylamino)-stibine (DMASb) represent a new family of reagents for growth of compound semiconductors.[4] These reagents are distinct from previously studied organometallic compounds due to their lack of direct group V–carbon or hydrogen bonds, and the presence of group V–nitrogen bonds. The molecules have been designed to circumvent problems of carbon incorporation often encountered in growth with trialkyl sources. They are also expected to have a relatively low decomposion temperature because of the weaker strength of the group V atom bond to nitrogen, as compared to the bond to carbon.[5] The tris(dimethylamino) reagents also represent the least bulky nitrogen-containing organometallic sources stable enough and with sufficiently high vapor pressures to be used in OMCVD.[6]

Metalorganic molecular beam epitaxy (MOMBE) studies by Abernathy et al.[7] have demonstrated that GaAs films, with no detectable carbon, may be grown at relatively low temperatures (~450 °C) without precracking when using trimethylgallium (TMG) and DMAAs. Mass spectroscopy investigations of reactions of DMAAs on GaAs surfaces under MOMBE conditions have shown that DMAAs is completely decomposed at temperatures as low as 450 °C.[8] Two major decomposition pathways were proposed, the first involving a simple scission of the arsenic–nitrogen bond, the second entailing a β-hydrogen elimination reaction to form either aziridine or methylmethyleneimine and absorbed surface hydrogen. The presence of hydrogen on the surface was believed to be important in reducing the carbon incorporation problem during the growth with TMG. These decomposition pathways have recently been confirmed by Xi et al. in temperature-programmed desorption (TPD) investigations.[9] Also, methylmethyl-

[†] Department of Chemistry.
[‡] Department of Chemical Engineering.
[⊗] Abstract published in *Advance ACS Abstracts,* February 15, 1995.

(1) Kuech, T. F.; Jensen, K. F. OMVPE of Compound Semiconductors. *Thin Film Processes-II*; Vossen, J. L., Kern, W., Eds.; Academic Press: San Diego, 1991.
(2) Stringfellow, G. B., *Organometallic Vapor Phase Epitaxy*; Academic Press: San Diego, 1989.
(3) Jones, A. C. *J. Cryst. Growth* **1993**, *129*, 728.
(4) Bohling, D. A.; Abernathy, C. R.; Jensen, K. F. *J. Cryst. Gowth*, **1994**, *136*, 118.
(5) Corbridge, D. E. C. *Phosphorous An Outline of its Chemistry, Biochemistry and Technology*, Elsevier: Amsterdam, 1990.
(6) Zimmermann, G.; Protzmann, H.; Marschner, T.; Zsebök, O.; Stolz, W.; Göbel, E.O.; Gimmnich, P.; Lorberth, J.; Filz, T.; Kurpas, P.; Richter, W. *J. Cryst. Growth* **1993**, *129*, 37.
(7) Abernathy, C. R.; Wisk, P. W.; Bohling, D. A.; Muhr, C. T. *Appl. Phys. Lett.* **1992**, *60*, 242; *J. Cryst. Growth* **1992**, *124*, 64.
(8) Salim, S.; Lu, J. P.; Jensen, K. F.; Bohling, D. A. *J. Cryst. Growth* **1992**, *124*, 16.

0897-4756/95/2807-0507$09.00/0

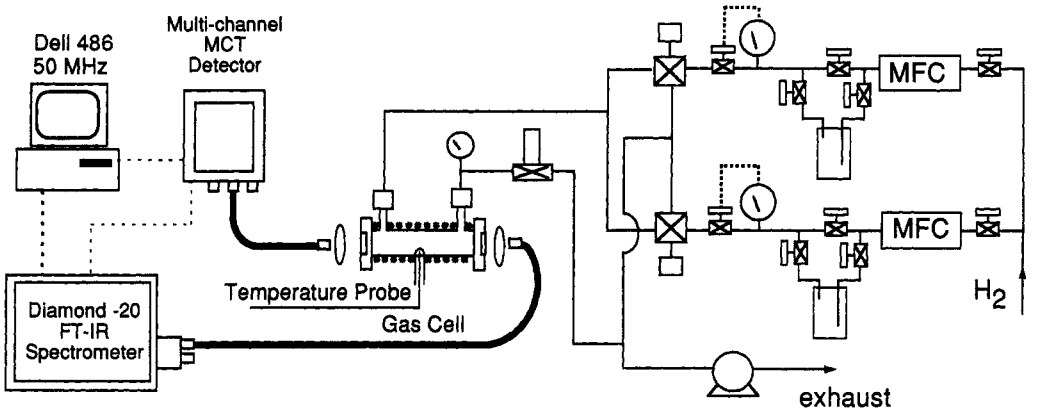

Figure 1. Schematic diagram of the fiber-optic-based FTIR spectrometer system.

eneimine has been established as the product of the surface β-hydrogen-transfer reaction.

OMCVD of GaAs with TMG and DMAAs in the temperature range 550–700 °C has been reported by Zimmer et al.[10] No nitrogen incorporation was detected in GaAs grown at 650 °C, while AlGaAs grown at 700 °C appeared to be contaminated by nitrogen. InP films grown by using trimethylindium (TMI) and DMAP were specular, with no detectable nitrogen or carbon incorporation.[6] The growth of InSb with TMI and DMASb, without significant impurity incorporation, has been reported as well.[11] In this contribution we explore the gas-phase decomposition of tris(dimethylamino) reagents at OMCVD conditions by using fiber-optics-based Fourier transform infrared (FTIR) and molecular beam mass spectroscopy.

Experimental Section

Fiber-Optics-Based FTIR Spectroscopy. The majority of the gas-phase reaction investigations were performed using the fiber-optics-based FTIR system (Galileo Electro-Optics Corp.) shown schematically in Figure 1. The spectrometer itself is a KVB Analect Diamond-20, with a resolution of 2 cm^{-1}. The system is controlled by a Dell 486-50 MHz computer. The IR emission from the interferometer is coupled into an optical fiber through a launcher. The optical fiber guides the infrared radiation to the sensing region, where the light is collimated into a 12 mm beam with a prealigned optical collimator module optimized for the mid-infrared. The collimated beam passes through the gas cell and is focused onto the return fiber with a second prealigned optical module. Angular adjustment on both collimators allows the optical throughput of the system to be optimized. A liquid-cooled, mid-IR mercury cadmium telluride (MCT) detector is used.

Two types of optical fibers were used: chalcogenide and fluoride fibers.[12] The former type is transparent in the spectral region 900–3300 cm^{-1} with limited transmission around 2200 cm^{-1}, whereas the latter has an operating window from 2200 to 20 000 cm^{-1}.

The experiments were performed in a Crystal Specialties OMCVD reactor system. The reactor was replaced by a gas cell designed for in situ monitoring of gas-phase decomposition. The cell (12.7 cm long) was constructed from a quartz tube (2.5 cm diameter), with quartz flanges fused to the tube ends (cf. Figure 1). CaF_2 windows with Viton O-ring seals were placed at each end and sealed with stainless steel flanges that were purged to minimize window deposits during the experiments. The cell could be uniformly heated to 650 °C with a resistive heater wrapped around the wall of the gas cell. The temperature was determined by inserting a type-K thermocouple into a thermocouple well penetrating into the gas cell.

The thermal decomposition studies were carried out at a reactor pressure of 600 Torr using H_2 (Matheson, 99.9995%), He (Airco, 99.999%), and D_2 (Matheson, 99%) as carrier gases. During experiments, the total flow of carrier gas to the reactor was maintained at 60 sccm, and the flow rate of the organometallic source was kept at 12 μmol/min. After each IR absorption measurement, the gas cell was evacuated and a reference spectrum recorded. An average of 128 scans at 4 cm^{-1} resolution was used for each spectrum.

Heat- and mass-transfer analyses showed that transport in the cell was dominated by diffusion under the conditions investigated. Residence time distribution studies at room temperature further showed that the system behaved as a well-mixed reactor.[13] Temperature and concentration profiles could therefore be assumed uniform across most of the cell width, except near infrared windows, which were cooled to a temperature of 50 °C. To interpret decomposition data, a simple two-cell reactor model was used, based on a well-mixed reactor section for the uniform temperature region, and a dead volume section for the region adjacent to the windows. This model was calibrated against published data for the pyrolysis of trimethylgallium (TMG) and trimetylindium (TMI).[14]

The gas cell was modified in the following manner to explore possible surface effects upon decomposition of the molecules. A tube of stainless steel wire cloth was inserted into the center of the gas cell to ensure an open IR beam path. Effects of SiO_2 on the decomposition were studied by inserting 4-mm-diameter borosilicate beads into the annular region between the gas cell and wire cloth. GaAs surface reactions were explored by inserting polycrystalline GaAs chips. Prior to loading the cell, both the SiO_2 and GaAs packing materials were degreased with trichloroethylene at 80 °C and rinsed in acetone and methanol. After placement in the cell, the GaAs chips were further treated in H_2 at elevated temperature (>400 °C) for 15 min to remove native oxides.

Molecular Beam Mass Spectrometer Investigations. The FTIR investigations were augmented by pyrolysis studies in a stagnation point OMCVD flow reactor equipped with molecular beam sampling through a pinhole in the substrate heater. This system has been used previously in decomposition studies of different organometallic reagents.[15] The gas was sampled through a 100 μm pinhole in a stainless steel foil in the center of a heated graphite susceptor. The sampled

(9) Xi, M.; Salim, S.; Jensen, K. F.; Bohling, D. A. *Mater. Res. Soc. Proc.* **1994**, *334*, 169. Xi, M.; Jensen, K. F. *Surf. Sci.*, in press.
(10) Zimmer, M. H.; Hovel, R.; Brysch, W.; Brauers, A.; Balk, P. *J. Cryst. Growth* **1991**, *107*, 348.
(11) Baucom, K. C.; Biefeld, R. M. *Appl. Phys. Lett.* **1994**, *64*, 3021.
(12) Driver, R. D.; Leskpwitz, G. M.; Curtiss, L. E. *SPIE* **1990**, *1228*, 233.
(13) Salim, S.; Jensen, K. F.; Driver, R. D. *Mater. Res. Symp. Proc.* **1994**, *324*, 241.
(14) Salim, S.; Lim, C. K.; Jensen, K. F.; Driver, R. D. *SPIE* **1994**, *2069*, 132.
(15) Lee, P. W.; Omstead, T. R.; McKenna; Jensen K. F. *J. Cryst. Growth* **1987**, *85*, 165.
(16) Maslowsky, E., Jr. *Vibrational Spectra of Organometallic Compounds*; Wiley Interscience: New York, 1977.

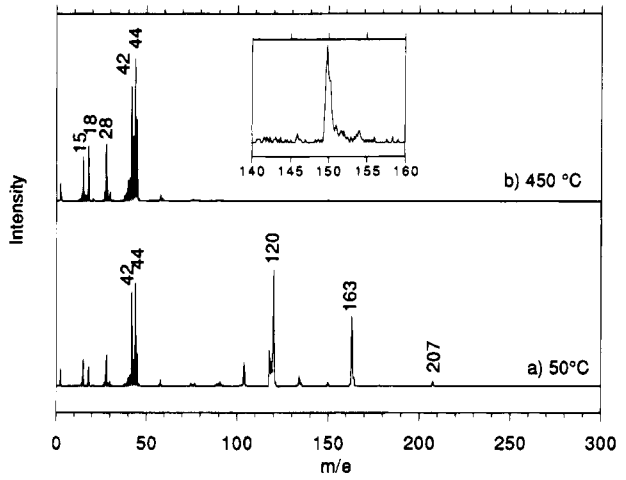

Figure 2. Molecular beam mass spectra of DMAAs at (a) 50 °C and (b) 450 °C.

gas stream was expanded into a molecular beam through two differentially pumped stages and collimated by a skimmer toward a Balzers 311 quadrupole mass spectrometer. This arrangement emulated conditions in a growth reactor and enabled in situ monitoring of gas-phase species in the reactor with minimal downstream gas-phase and wall interactions. Additional details about the system have been reported previously.[15]

The mass spectroscopy pyrolysis studies of the dimethylamino reagents served to verify and to complement results obtained by the infrared technique. The system played a special role in identification of decomposition products, with infrared signatures in the infrared region below 1000 cm^{-1}, which could not be accessed in the fiber-optics-based FTIR setup. The pyrolysis studies were conducted with H_2 as a carrier gas, at a flow rate of 20 sccm. The reactor was maintained at 30 Torr; the delivery rate of the organometallic reagents was set at 20 μmol/min.

Organometallic Sources. DMAP, DMAAs, and DMASb (Air Products and Chemicals) were electronic grade and supplied in stainless steel bubblers. The vapor pressures at the bubbler temperature of 40 °C were 6.9, 5, and 4.0 Torr for DMAP, DMAAs, and DMASb, respectively.

Results

Decomposition of DMAAs. Typical mass spectra of DMAAs in H_2 carrier gas at 30 Torr are shown in Figure 2 for two different temperatures: T = 50 °C, where no decomposition has occurred; T = 450 °C, after the decomposition has been completed. The low-temperature spectrum displays peaks at m/e = 207, corresponding to the parent molecule, at m/e =163, representing $[(CH_3)_2N]_2As^+$, and at m/e = 120, corresponding to $[(CH_3)_2N]AsH^+$. The fragmentation pattern of DMAAs is similar to that reported for DMAP.[17] Table 1 gives the characteristic peaks for the three tris(dimethylamino) reactants.

At the high temperature, the parent peaks at m/e = 207, 163, and 120 disappear and no products with m/e > 75 appear except for a peak at m/e = 150, corresponding to As_2. This behavior indicates that the DMAAs decomposes cleanly to As, without the formation of any organometallic As byproducts. As_4 would also be expected as a product, but its mass falls outside the range of the mass spectrometer.

The major products at 450 °C are those of m/e = 42 and 44. The assignment of the peaks to 44 to dimethylamine and 42 to aziridine or methylmethyleneimine, have been discussed by Salim et al.[8] The peak at m/e = 15 is assigned to methyl groups originating from the fragmentation of dimethylamine, methylmethyleneimine, and methane. Further identification of the decomposition products is achieved by augmenting the mass spectroscopy data with FTIR observations.

FTIR spectra of DMAAs in H_2 at 600 Torr at three different temperatures are shown in Figure 3. The high-temperature spectra are corrected spectra after subtracting the contribution due to the absorption in the dead volume region adjacent to the windows. The low temperature spectrum, taken at 200 °C, gives the vibrational frequencies of the DMAAs molecule. The complete IR assignments for DMAAs, DMAP,[18] and DMASb are summarized in Table 2. As the temperature of the gas cell is increased to 430 °C, significant changes in the vibrational spectrum are observed corresponding to the decomposition of the molecule. As the pyrolysis proceeds, the distribution of peaks in the C–H vibrational stretching region, 2800–3000 cm^{-1}, loses distinct features and becomes a broad adsorption. New

Table 1. Assignments for Major Peaks in DMAP, DMAAs, and DMASb Mass Spectra

DMAP		DMAAs		DMASb[a]	
m/e	assignment	m/e	assignment	m/e	assignment
163	$[(CH_3)_2N]_3P^+$	207	$[(CH_3)_2N]_3As^+$	252, 254	$[(CH_3)_2N]_3Sb^+$
119	$[(CH_3)_2N]_2P^+$	163	$[(CH_3)_2N]_2As^+$	208, 210	$[(CH_3)_2N]_2Sb^+$
76	$[(CH_3)_2N]HP^+$	120	$[(CH_3)_2N]HAs^+$	165, 167	$[(CH_3)_2N]HSb^+$
60	$[(CH_3)N]P^+$	104	$[(CH_3)N]As^+$	120, 122	Sb^+
44	$(CH_3)_2N^+$	44	$(CH_3)_2N^+$	44	$(CH_3)_2N^+$
42	$(CH_2)_2N^+$	42	$(CH_2)_2N^+$	42	$(CH_2)_2N^+$
28	CH_2N^+	28	CH_2N^+	28	CH_2N^+
15	CH_3^+	15	CH_3^+	15	CH_3^+

[a] Sb has two significant isotopes (at m/e = 120 and 122).

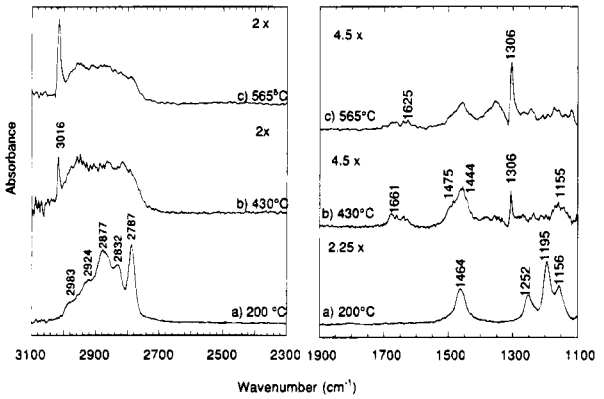

Figure 3. Infrared spectra of DMAAs in H_2 at (a) 200 °C, (b) 430 °C, and (c) 565 °C. Spectra b is after subtracting the parents' contribution.

Table 2. Assignment of Major Bands in Infrared Spectra for DMAP, DMAAs, and DMASb

wavenumber (cm^{-1})			
DMAP	DMAAs	DMASb	assignment
1080	1058	1065	$\varrho(CH_3)$
1169	1156	1163	$\varrho(CH_3)$
1203	1195	1185	$\varrho(CH_3)$
1280	1252	1248	$\nu_{ass}(C-N-C)$
1460	1464	1464	$\delta(CH_3)$

(17) Borer, W. Z.; Cohn, K. *Anal. Chim. Acta* **1969**, 47, *355*.

(18) Shagidullum, R. R., Chemova, A. V., Vvnogradava, V. S., Mukhametov, F. S., Eds. *Atlas of IR Spectra of Organophosphorous Compounds*; Nauka Publishers, Kluwer Academic Publishers: Dordrecht, 1990.

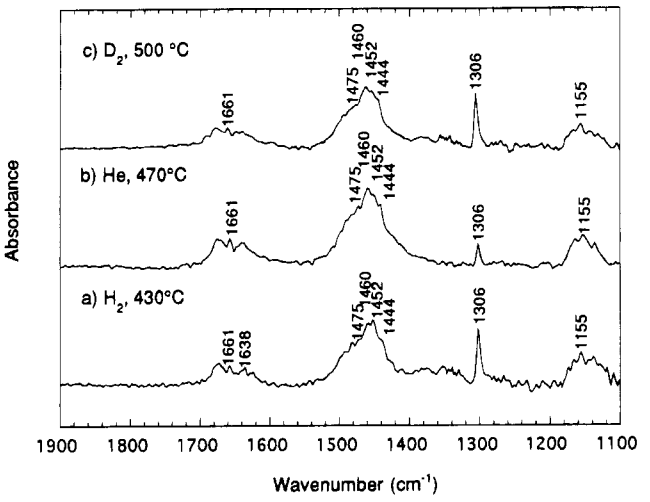

Figure 4. Infrared spectra of decomposition products of DMAAs in (a) H2, (b) He, and (c) D_2.

Table 3. Infrared Bands for Pyrolysis Products

name	wavenumber (cm^{-1})	assignment
dimethylamine	1462	$\delta(CH_3)$
	1155	$\varrho(CH_3)$
	1020	$\varrho(CH_3)$
methylmethyleneimine	1661	$\nu(C{=}N)$
	1475	$\delta(CH_2)$
	1444	$\delta(CH_3)$
	1220	$\varrho(CH_3)$
	1026	$\varrho(CH_3)$
methyleneimine	1638	$\nu(C{=}N)$
	1453	$\delta(CH_2)$
	1342	$\delta(CNH)$
	1055	$\varrho(CH_2)$
methane	3016	$\nu_3(CH_4)$
	1306	$\nu_4(CH_4)$
ammonia	3444	$\nu_3(NH_3)$
	1626	$\nu_4(NH_3)$
phosphine	2323	$\nu_1(PH_3)$

peaks are observed at 1600−1700 cm^{-1}, the peak shape at 1400−1500 cm^{-1} changes in appearance, and peaks at 1195 and 1250 cm^{-1} disappear, while the peak centered around 1155 cm^{-1} remains intact.

The 1155 cm^{-1} signature is assigned to the CH_3 deformation band of dimethylamine.[19] Additional evidence of the presence of this product is the CH_3 bending mode at 1460 cm^{-1} (Figure 4). The mode for N−H stretching vibration is not detected because of its weak IR cross section.[19]

The second product observed at 430 °C is methylmethyleneimine. The spectra shown in Figures 4 and 5 display a sharp peak centered at 1660 cm^{-1} and broad shoulders at around 1676 and 1640 cm^{-1} stemming from the C=N stretching vibrational rotational mode of methylmethyleneimine.[20] The spectra at 450 °C further reveal two peaks at 1475 and 1444 cm^{-1}, corresponding to the CH_2 and CH_3 bending modes of methylmethyleneimine. Vibrational modes of aziridine[21] are not detected, which suggests that the $m/e = 42$ peak in the molecular beam mass spectrum represents the formation of methylmethyleneimine and *not* the presence of aziridine.

(19) Schrader, B., Ed. *Raman / Infrared Atlas of Organic Compound*; VCH: New York, 1989.
(20) Stolkin, I.; Ha, T. K.; Günthard, Hs. H. *Chem. Phys.* **1977**, *21*, 327.
(21) Schmanouchi, T. *Table of Molecular Vibrational Frequencies Consolidated*; NSRDS, Washington, DC, 1972; Vol. 1, and references therein.

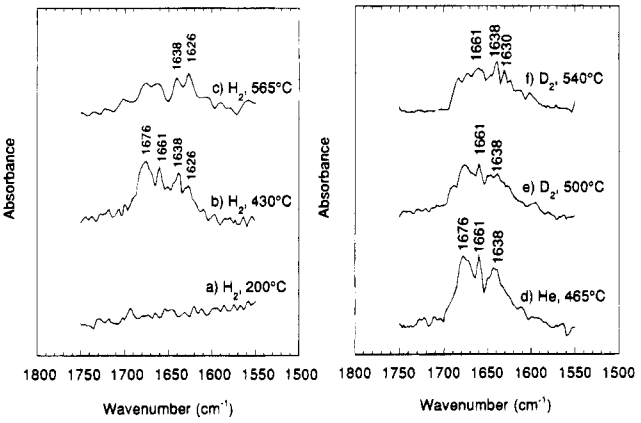

Figure 5. Expanded view of infrared spectra of DMAAs in (a) H_2 at 200 °C, (b) H_2 at 430 °C, (c) H_2 at 565 °C, (d) He at 465 °C, (e) D_2 at 500 °C, and (f) D_2 at 540 °C.

Methyleneimine is also detected by the appearance of peaks at 1638 cm^{-1} attributed to the C=N vibrational mode and a peak at 1453 cm^{-1} corresponding to the CH_2 bending modes of the molecule.[22] The N−H vibrational mode of the imine at 3400 cm^{-1} was again not detected because of its weak infrared adsorptivity. Methane, represented by sharp peaks at 3016 and 1306 cm^{-1}, is observed as well at this temperature.[21,23]

When the pyrolysis temperature is further increased to 565 °C, new gas-phase reaction products are formed as evidenced in the top spectra of Figure 3. Methane is increased. The formation of dimethylamine and methylmethyleneimine is reduced, and a new weak peak at 1625 cm^{-1} emerges (see Figure 5). This peak is assigned to deformation stretching of NH_3.[21,23] The assignment of ammonia is supported by the simultaneous appearance in fluoride fiber experiments of another band at 3334 cm^{-1} (not shown), representing vibrational stretching of the molecule.

Figure 6a shows variations in characteristic peak intensities for the products as a function of temperature. IR signals were normalized with respect to their maximum value and corrected for possible absorption by unreacted parent molecules in the low-temperature region adjacent to the IR windows. Absorption at 1195 cm^{-1} was used to represent the parent molecule, since none of the decomposition products had strong vibrational modes in this spectral region. Methane, methylmethyleneimine, and methyleneimine are represented by bands at 1306, 1661, and 1638 cm^{-1}, respectively. Dimethylamine is followed by the absorption intensity at 1155 cm^{-1} after subtraction of contributions from the parent reagent.

DMAAs decomposition was also done in He carrier gas. Dimethylamine (1155 cm^{-1}), methylmethyleneimine (1661 cm^{-1}), methyleneimine (1638 cm^{-1}), and methane (1306 cm^{-1}) were again the major products, as shown in Figures 4 and 5. However, no absorption at 1625 cm^{-1} by NH_3 was detected. This behavior would be expected since no excess hydrogen would be available for the formation of ammonia during the pyrolysis of dimethylamine.

Figure 6b shows the normalized intensities of the pyrolysis products in He as functions of decomposition

(22) Hamada, Y.; Hashiguchi, K.; Tsuboi, M.; Koga, Y.; Kondo, S. *J. Mol. Spectrosc.* **1984**, *105*, 70.
(23) Herzberg, G. *Infrared and Raman Spectra of Polyatomic Molecules*; Van Nostrand: New York, 1945, and references therein.

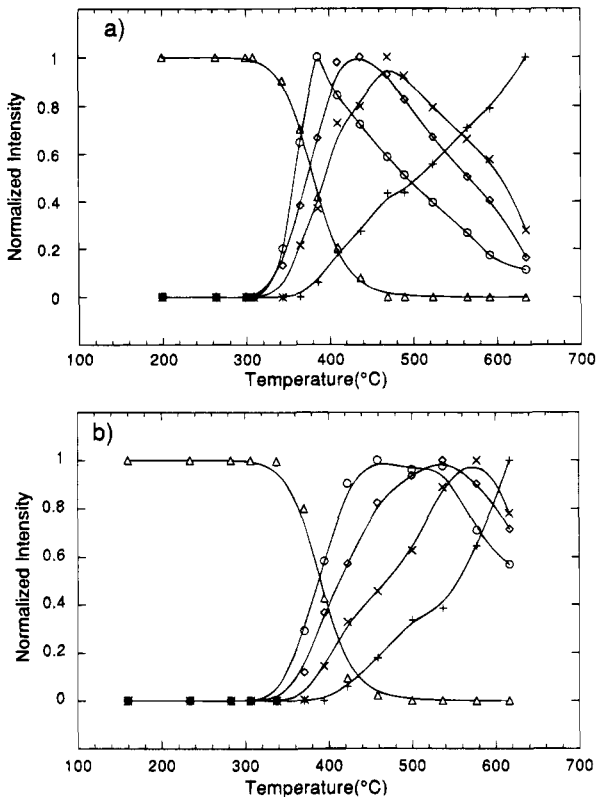

Figure 6. Decomposition products of DMAAs in (a) H_2, and (b) He: (△) parent molecule, (○) dimethylamine, (+) methane, (×) methyleneimine, and (◇) methylmethyleneimine. Table 4 lists the ratio of maximum intensity of the products with respect to that for the parent molecules.

Table 4. Comparison of Relative Peak Intensities for Decomposition Products and Parents in H_2 and He

compound	products	in H_2	in He
DMAAs	parent	1.00	1.00
	dimethylamine	0.25	0.18
	methylmethyleneimine	0.12	0.13
	methyleneimine	0.12	0.10
	methane	1.15	0.30
DMAP	parent	1.00	1.00
	dimethylamine	0.10	0.05
	methylmethyleneimine	0.09	0.09
	methyleneimine	0.09	0.09
	methane	0.76	0.22
DMASb	parent	1.00	1.00
	dimethylamine	0.22	0.20
	methylmethyleneimine	0.12	0.15
	methyleneimine	0.10	0.10
	methane	0.76	0.19

temperature. The same IR adsorption bands as in the H_2 case (Figure 6a) are used to represent the decomposition products. Table 4 summarizes the relative peak intensities of the maximum product with respect to the parent molecule. Comparison of Figures 6a and 6b reveals that the decomposition temperature, corresponding to 50% conversion, is 25 °C lower in H_2 carrier gas than in He. In addition, from Table 4, concentrations of dimethylamine and methane are much less in He than those observed in H_2. Dimethylamine, methylmethyleneimine, and methyleneimine intensities also begin to decrease at lower temperature in H_2 as compared to He. These observations, in particular the shift in product distribution, suggest that hydrogen radical reactions play an important role in the gas-phase decomposition mechanisms.

Reduced IR transmissivity around 2200 cm^{-1} because of Se−H absorption bands in the fiber material limits the observation of vibrational modes around 2200 cm^{-1}; specifically, As−H, which would be a product from a β-hydrogen transfer reaction.[21,23] To explore the potential formation of AsH, decomposition experiments were also carried out using D_2.

The use of the isotope is expected to shift the As−H band out of the 2200 cm^{-1} window to AsD vibrational modes at 1523 cm^{-1}. The spectra of DMAAs in D_2 at 500 °C are shown in Figure 4, and an expanded view of the spectra region at 1600−1700 cm^{-1} is shown in Figure 5. The spectra are nearly identical to those collected in H_2 and He ambients, and there is no evidence of deuterated arsine vibrational modes at 1523 cm^{-1}. The CH_3 bond deformation of dimethylamine [$(H_3C)_2NH$] and possibly N-deuterated dimethylamine [$(H_3C)_2ND$] are observed at 1155 cm^{-1}. Unfortunately, the N−D and N−H bands for dimethylamine are so weak that they could not be detected by the existing experimental setup.[19] Methane (CH_4) absorption at 1306 cm^{-1}, methylmethyleneimine at 1661 cm^{-1}, and methyleneimine at 1638 cm^{-1} are also observed. When the temperature is increased to 540 °C, a new vibrational mode emerges at 1630 cm^{-1}, as shown in Figure 5. This mode is assigned to the C=N stretching of deuterated methyleneimine (H_2C=ND) as reported by Hamada.[22]

CH_3D is also observed as a reaction product at high temperature. One of the differences between spectra of CH_3D and CH_4 is the appearance of a new sharp peak at 1155 cm^{-1} due to CH_3 deformation vibrations of CH_3D.[23] This vibrational mode is easily distinguished compared to those of dimethylamine, which feature triplet peaks centered at 1155 cm^{-1}.[19] The C−D stretching vibrational mode of the molecule cannot be observed in the present fiber setup since the adsorption band is located in the cutoff region of the chalcogenide fiber, ~2200 cm^{-1}.

The N−D vibrational modes of deuterated amine species (NH_xD_{3-x}) is not observed in the spectra at high temperature, which may be rationalized in terms of the combination of a weak infrared cross section, a low concentration of the species. By comparison, the intensity of the NH_3 signal detected for pyrolysis in H_2, using the equivalent vibrational mode at 1625 cm^{-1}, is very weak and close to the minimum detection limit.

Decomposition of DMAP. Molecular beam mass spectra of DMAP in 30 Torr of H_2 at cell temperatures of 50 and 450 °C are shown in Figure 7. The fragmentation pattern of DMAP has been reported in the literature,[17] and a summary of the peak assignments is given in Table 1. At 450 °C, the intensity of the peaks from the parent molecules (m/e = 60, 76, 120, and 163) are reduced significantly, reflecting decomposition of the parent molecule. The major reaction products are, as in the case of DMAAs, methylmethyleneimine and dimethylamine with characteristic signals at m/e = 42 and m/e = 44, respectively. P_2 (m/e = 62) and P_4 (m/e = 124) are also observed, but no evidence of organophosphine intermediates is found.

As in the case of DMAAs, the gas-phase pyrolysis of DMAP was investigated by FTIR at 600 Torr in H_2, D_2, and He ambients. The spectra for decomposition of DMAP in H_2 are shown in Figure 9. The peak assign-

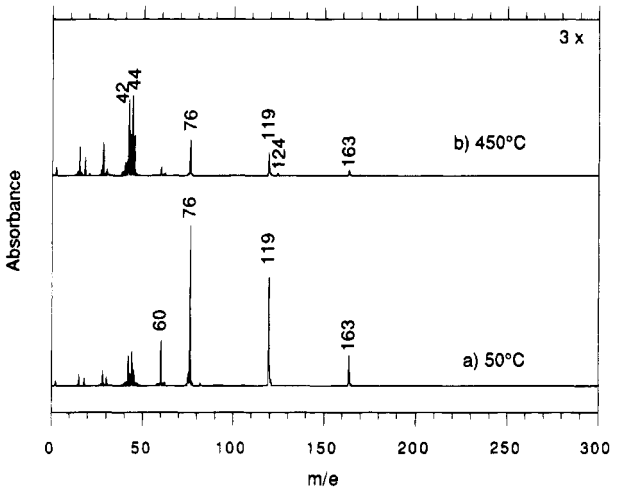

Figure 7. Molecular beam mass spectra of DMAP at (a) 50 °C and (b) 450 °C.

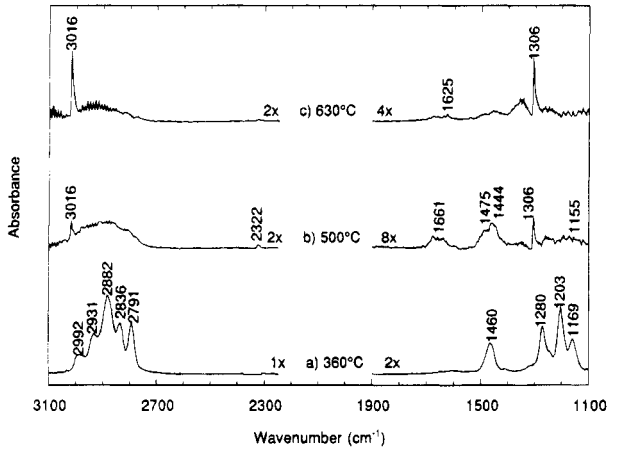

Figure 8. Infrared spectra of DMAP in H_2 at (a) 360 °C, (b) 500 °C, and (c) 630 °C. Spectra b is after subtracting the parents' contribution.

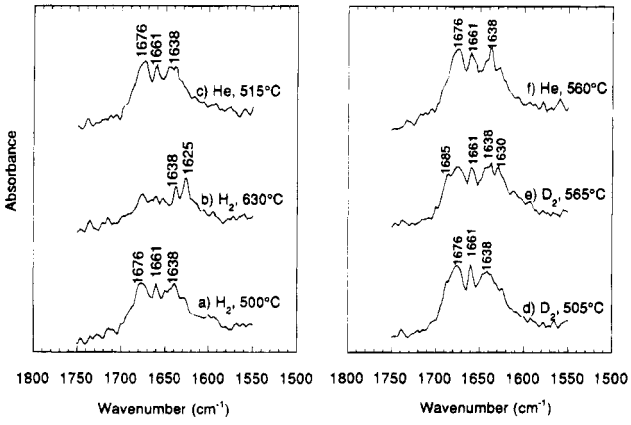

Figure 9. Expanded view of infrared spectra of DMAP in (a) H_2 at 500 °C, (b) H_2 at 630 °C, (c) He at 515 °C, (d) D_2 at 505 °C, (e) D_2 at 565 °C, and (f) He at 560 °C.

ment for the DMAP molecule follows that of DMAAs and is given in Table 2. The spectra recorded at 500 °C show a decrease in the relative intensities of the bands at 1204 and 1155 cm^{-1} as a result of the decomposition of the parents (1204 cm^{-1}) and the formation of dimethylamine (1155 cm^{-1}). Methane with the sharp bands at 1306 and 3016 cm^{-1} is observed. The presence of the product methylmethyleneimine is also apparent by absorptions at 1661, 1444, and 1475 cm^{-1}.

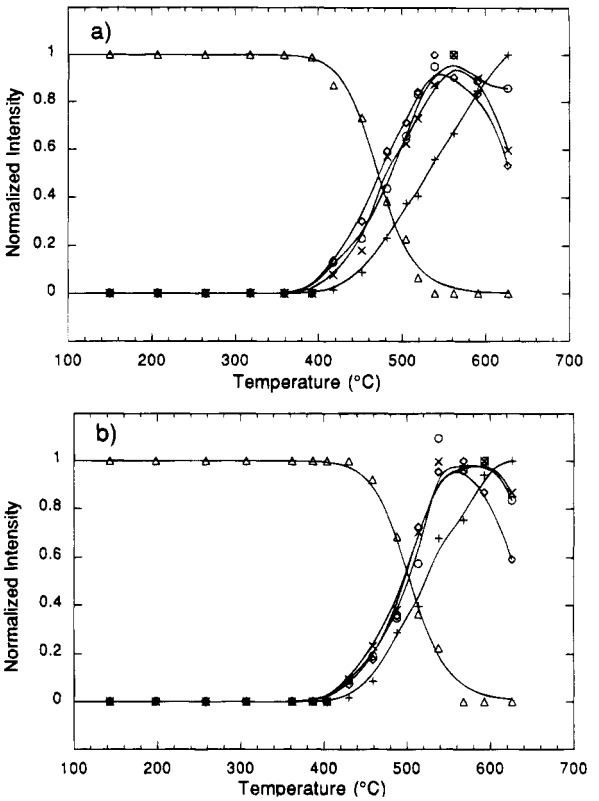

Figure 10. Decomposition products of DMAP in (a) H_2, and (b) He: (△) parent molecule, (○) dimethylamine, (+) methane, (×) methyleneimine, and (◇) methylmethyleneimine. Table 4 lists the ratio of maximum intensity of the products with respect to that for the parent molecules.

An expanded view of the spectral region 1600–1700 cm^{-1} (Figure 10) reveals the presence of the C=N vibration mode of methyleneimine at 1638 cm^{-1}. Further increasing the temperature to 630 °C leads to the formation of more methane and a new peak at 1625 cm^{-1} corresponding to NH_3.

At temperatures exceeding 500 °C, a new absorption band, centered at 2322 cm^{-1} is observed (Figure 8). The peak position and the shape resemble that of the PH_3 molecule vibrational mode.[23] The signal is stronger than that for NH_3 because the observed vibrational mode of PH_3 at 2322 cm^{-1} has approximately a 6 times larger infrared cross section.[24] In D_2 ambient (Figures 10 and 11), the peak position remains the same, but the peak shape is different and considerably weakened. Moreover, a new band appears at 1685 cm^{-1} that is not observed for decomposition in H_2 and He. This spectral position is very close to that reported for P–D vibrational bands of PH_2D,[25] indicating the formation of PD_xH_{3-x} ($x = 1$ or 2) during pyrolysis in D_2. Deuterated methyleneimine (H_2C=ND) and CH_3D are again observed as products of the gas-phase reactions.

Figures 10a and b show the decomposition products in H_2 and He, respectively, as a function of the gas-phase temperature. The reagent and products are characterized by vibrational modes equivalent to those used in the case of DMAAs. In both gases, dimethylamine, methylmethyleneimine, methyleneimine, and methane appear as soon as the reactant starts to decompose. Decomposition in He leads to the formation

(24) McKean, D. C.; Schatz, P. N. *J. Chem. Phys.* **1956**, *24*, 316.
(25) Kshirsagar, R. J.; Job, V. A. *J. Mol. Spectrosc.* **1993**, *161*, 170.

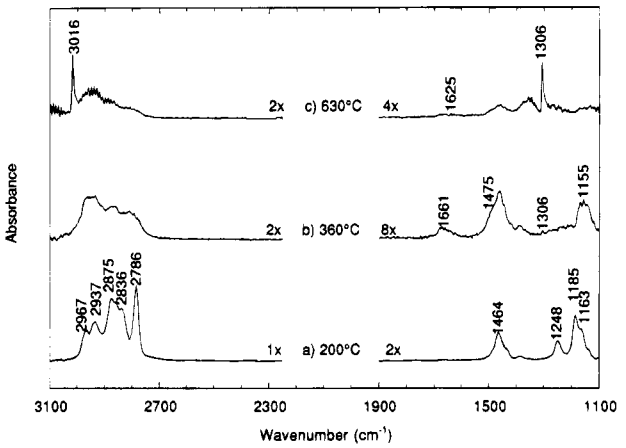

Figure 11. Infrared spectra of DMASb in H_2 at (a) 200 °C, (b) 360 °C, and (c) 630 °C. Spectra b is after subtracting the parents' contribution.

of less dimethylamine and methane. No evidence for the formation of PH_3 is observed for gas-phase decomposition of DMAP in He.

Decomposition of DMASb. Decomposition studies of DMASb were carried out solely in the FTIR fiber setup. Spectra of DMASb in H_2 at 200, 360, and 630 °C are shown in Figure 11. The 200 °C spectrum represents DMASb before decomposition. Peak assignments are given in Table 2, and they are equivalent to those for DMAAs and DMAP. When the temperature is increased to 360 °C, DMASb decomposes, partially producing methylmethyleneimine (1661, 1444, and 1475 cm^{-1}), dimethylamine (1155 and 1460 cm^{-1}), and methane (1306, 3016 cm^{-1}) analogous to the pyrolysis of DMAAs and DMAP. At 630 °C, the concentrations of dimethylamine and methylmethyleneimine are reduced with additional formation of methane and ammonia. In D_2, deuterated methyleneimine (1630 cm^{-1}) and CH_3D are again detected as in the pyrolysis of the other tris(dimethylamino) sources.

Normalized variations in reagents and product concentrations with temperature are summarized in Figure 12. In H_2, dimethylamine and methylmethyleneimine are produced as the reagent starts to decompose. Methane and methyleneimine start to pick up production at around 400 °C, and ammonia is generated at temperature above 550 °C. The study of gas-phase pyrolysis in He shows that the start of decomposition occurs ~25 °C higher than in H_2. There is less production of methane and dimethylamine, and no formation of ammonia similar to those observed in DMAAs and DMAP.

Discussion

Gas-Phase Pyrolysis Pathways of Tris(dimethylamino) Group V Reagents. The decomposition mechanism, shown schematically in Figure 13, is consistent with the experimental data. The relative widths of the reaction arrows from the tris(dimethylamino) reagent are used to indicate the importance of the reaction. The gas-phase decomposition of the molecules is initiated and dominated by the homolysis reaction

$$((CH_3)_2N)_3E \rightarrow ((CH_3)_2N)_2E + (CH_3)_2N^{\bullet} \quad (1)$$

where E represents P, As, or Sb. A comparison between

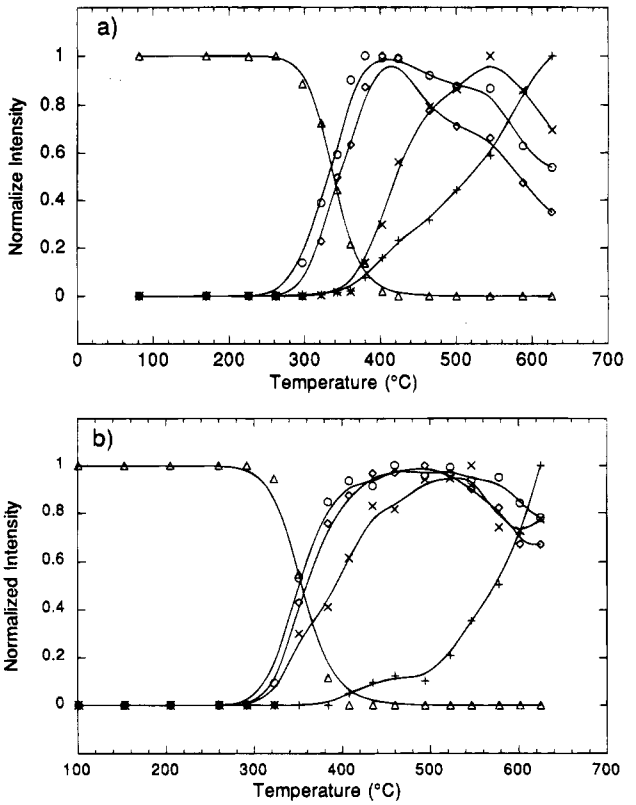

Figure 12. Decomposition products of DMASb in (a) H_2, and (b) He: (△) parent molecule, (○) dimethylamine, (+) methane, (×) methyleneimine, (◇) methyl-methyleneimine. Table 4 lists the ratio of maximum intensity of the products with respect to that for the parent molecules.

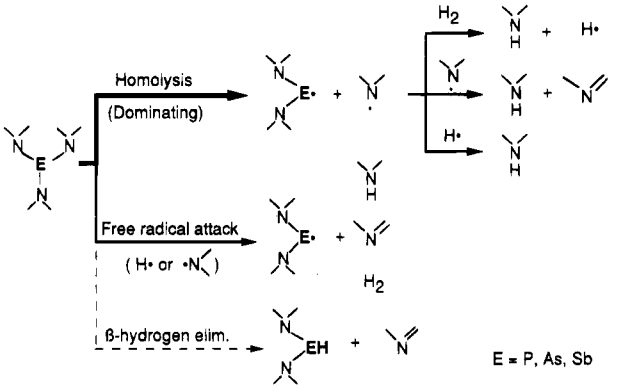

Figure 13. Schematic of gas-phase decomposition pathways for $[(CH_3)_2N]_3E$, E = P, As, and Sb.

the degree of decomposition of DMAAs, DMAP, and DMASb as a function of temperature is given in Figure 14. With increasing temperature, DMASb decomposes first, followed by DMAAs, and at higher temperatures, DMAP. This trend in decomposition temperature is consistent with the bond strength of N−E being weakest for E = Sb and strongest for E = P.

The continuous curves in the graph represent the fitted model based on an analysis of a first-order decomposition reaction in a well-mixed reactor. The corresponding activation energies are summarized in Table 5. The same preexpontial factor of 10^{-13} s^{-1} was assumed for all three pyrolysis reactions since the fit to data did not provide statistically significant differences between the individual preexponential factors. The value of 10^{-13} s^{-1} is consistent with simple transition-state considerations. The activation energy for

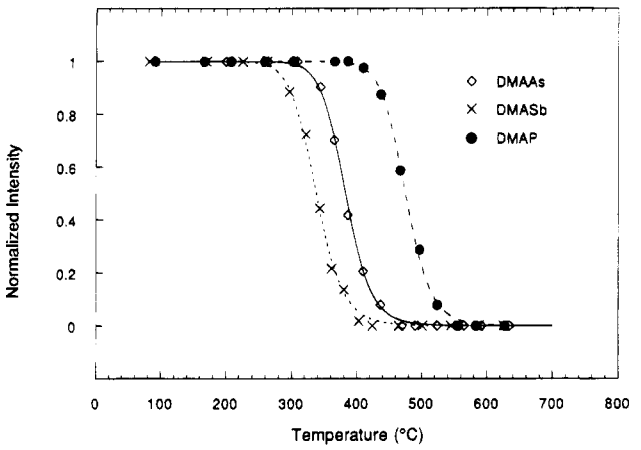

Figure 14. Comparison of decomposition profiles for DMAP, DMAAs, and DMASb. Points represent experimental data; curves are computed on the basis of first-order kinetics (cf. Table 5).

Table 5. Activation Energies for First-Order Decomposition of the Tris(dimethylamino) Reagents

	DMAP	DMAS	DMASb
E_a (kcal/mol)	50.6	44.0	41.1

pyrolysis of DMAP is very close to the reported P–N bond energy of 55 kcal/mol,[5] which indicates that the rate-limiting step in the gas-phase decomposition is the homolysis of the N–P bond.

For each reagent, decomposition commences at lower temperatures in H_2 than in He. Moreover, the amounts of dimethylamine and methane generated in a H_2 ambient are larger than those observed in He carrier gas. These observations suggest involvement of hydrogen radicals in a secondary decomposition path (see Figure 13). In the presence of H_2, the dimethylaminyl radical, formed in the homolysis reaction (1), abstracts H and produces a hydrogen radical:

$$(CH_3)_2N^{\bullet} + H_2 \rightarrow (CH_3)_2NH + H^{\bullet} \quad (2)$$

The H• radical can then further accelerate the decomposition of the amino reagent according to reactions of the form

$$((CH_3)_2N)_xE + H^{\bullet} \rightarrow ((CH_3)_2N)_{x-1}E + (CH_3)_2NH, \quad x = 1, 2, 3 \quad (3a)$$

$$((CH_3)_2N)_xE + H^{\bullet} \rightarrow ((CH_3)_2N)_{x-1}E + H_2 + H_2C{=}NCH_3, \quad x = 1, 2, 3 \quad (3b)$$

Analogous reactions take place in D_2 with the formation of deuterium radicals and subsequent attack on the amino reagent.

Dimethylaminyl radicals can also themselves accelerate decomposition of the molecule via the reaction

$$((CH_3)_2N)_xE + (CH_3)_2N^{\bullet} \rightarrow ((CH_3)_2N)_{x-1}E + (CH_3)_2NH + H_2C{=}NCH_3 \quad (4)$$

The participation of H• in the pyrolysis through reactions 2 and 3a is apparent in the increased amount of dimethylamine relative to methylmethyleneimine in H_2 as compared to He. The effect is particularly noticeable for pyrolysis of DMAAs, where ~1.5 times more dimethylamine is produced than in He,

The other possible channel for production of dimethylamine and methylmethyleneimine in both H_2 and He is the disproportional reaction

$$(CH_3)_2N^{\bullet} + (CH_3)_2N^{\bullet} \rightarrow (CH_3)_2NH + H_2C{=}NCH_3 \quad (5a)$$

This pathway is important in reactions involving dimethylaminyl radicals generated in photolysis and pyrolysis of nitrogen-containing compounds such as tetramethyl-2-tetrazene, trimethylamine, dimethylamine, and tetramethylhydrazine.[27]

A potential competing step to reaction 5a is the recombination of two dimethylaminyl radicals to produce tetramethylhydrazine (TMH):

$$(CH_3)_2N^{\bullet} + (CH_3)_2N^{\bullet} \rightarrow (CH_3)_2N{-}N(CH_3)_2 \quad (5b)$$

No TMH was detected as the products of decomposition of trimethylamino compounds in He, H_2, or D_2. Using the very low-pressure pyrolysis technique, Lazarou and Papagiannakopolos,[30] determined the rate constant for reactions 5a and 5b to be

$$k_{5a} = (4.10 \pm 0.52) \times 10^{-12}\ \text{cm}^3\ \text{molecule}^{-1}\ \text{s}^{-1}$$

$$k_{5b} = (1.70 \pm 0.19) \times 10^{-12}\ \text{cm}^3\ \text{molecule}^{-1}\ \text{s}^{-1}$$

respectively, at room temperature. Since the reactions have no activation barrier, the rate constant data predict the reaction 5a to be more than twice as fast as the recombination reaction 5b. Simulation of pyrolysis of TMH for the present experimental conditions with the use of reported kinetic data[28,29] reveals that TMH decomposes at temperatures similar to those required to pyrolyze the organometallic reagents. Thus, it is unlikely that TMH will be a stable pyrolysis product.

Additional reactions of the dimethylaminyl radical include a recombination reaction with hydrogen radicals to produce dimethylamine, or a hydrogen abstraction reaction to produce methylmethyleneimine, as observed in the very low-pressure pyrolysis of methylhydrazine:[29]

$$(CH_3)_2N^{\bullet} + H^{\bullet} \rightarrow (CH_3)_2NH \quad (6)$$

$$(CH_3)_2N^{\bullet} \rightarrow H_2C{=}NCH_3 + H^{\bullet} \quad (7)$$

$$(CH_3)_2N^{\bullet} + RH \rightarrow (CH_3)_2NH + R^{\bullet} \quad (8)$$

where H is any organic H-donor molecules.

At temperatures higher than 400 °C, the dimethylaminyl radical decomposes to form a methyl radical and methyleneimine[27] according to

(26) Trotman-Dickerson, A. F.; Milne, G. S. *Table of Bimolecular Gas Reactions*; NSRDS: Washington, DC, 1969.
(27) Seetula, J.; Kalliorinne, K.; Koskikallio, J. *J. Photochem. Photobiol.* **1988**, *A43*, 31.
(28) Patai, S., Ed. *The Chemistry of Amino, Nitroso and Nitro Compounds and Their Derivatives Part 1*; John Wiley & Sons: New York, 1982.
(29) Golden, D. M.; Solly, R. K.; Gac, N. A.; Benson, S. W. *Int. J. Chem. Kinet.* **1972**, *4*, 433.
(30) Lazarou, Y. L.; Papagiannakopoulos, P. *J. Phys. Chem.* **1993**, *97*, 9133.

$$(CH_3)_2N^{\bullet} \rightarrow CH_3^{\bullet} + H_2C{=}NH \quad (9)$$

This reaction is responsible for the formation of methyleneimine in decomposition under He. N-deuterated methyleneimine ($H_2C{=}ND$), which is observed in D_2 ambients, is likely generated in a radical exchange reaction of D with methylmethyleneimine:

$$H_2C{=}NCH_3 + D^{\bullet} \rightarrow H_2C{=}ND + CH_3^{\bullet} \quad (10)$$

This reaction does not take place in He. As a consequence, the formation of methylmethyleneimine is observed up to 550 °C in He, in contrast to H_2 and D_2 cases where the methylmethyleneimine concentration begins to decrease at temperatures as low as 425 °C.

The methyl radical formed in reactions 9 and 10 participates in abstraction and recombination reactions to yield methane:

$$CH_3^{\bullet} + H_2 \rightarrow CH_4 + H^{\bullet} \quad (11)$$

$$CH_3^{\bullet} + H^{\bullet} + M \rightarrow CH_4 + M \quad (12)$$

$$CH_3^{\bullet} + RH \rightarrow CH_4 + R^{\bullet} \quad (13)$$

$$CH_3^{\bullet} + (CH_3)_2N^{\bullet} \rightarrow CH_4 + H_2C{=}NCH_3 \quad (14)$$

Reactions 11 and 12 are primarily responsible for the formation of methane in H_2, whereas reactions 13 and 14 are the primary sources of methane in He.

The recombination reaction:

$$CH_3^{\bullet} + (CH_3)_2N^{\bullet} \rightarrow (CH_3)_3N \quad (15)$$

to form trimethylamine could potentially compete with reaction 14, but no trimethylamine reaction is observed as a reaction product in the decomposition. At the elevated temperatures, it is very likely that the recombination reaction 15 proceeds at a slower rate than the disproportional reaction 14, similar to the case of reactions 5b and 5a for the dimethylaminyl radicals. Trimethylamine is reported to decompose to methane and methylmethyleneimine through a first-order process with $10^{14.3}e^{-29.5/T}$ s^{-1}.[31] Simulations of decomposition in the present gas cell shows trimethylamine to decompose completely in the temperature range 500–600 °C. It is therefore not expected to be a major product of the pyrolysis product.

At temperatures exceeding 550 °C, homolysis of the N–C bond commences, as evidenced by decreases in concentrations of methylmethyleneimine, methyleneimine, and dimethylamine, along with the continual increase in the production of ammonia at elevated temperatures. The process is probably initiated by the pyrolysis of dimethylamine and dimethylaminyl radicals. The decomposition of dimethylamine has been reported to follow first-order kinetics with activation energy of 46.6 kcal and preexponential factor of $10^{10.5}$ s^{-1}.[28] Simulation of the degree of decomposition of dimethylamine under the current gas-cell conditions shows that the compound starts to decompose at temperatures as low as 550 °C.

(31) Kauffman, R. G. Ph.D. Thesis, Catholic University of America, 1962.

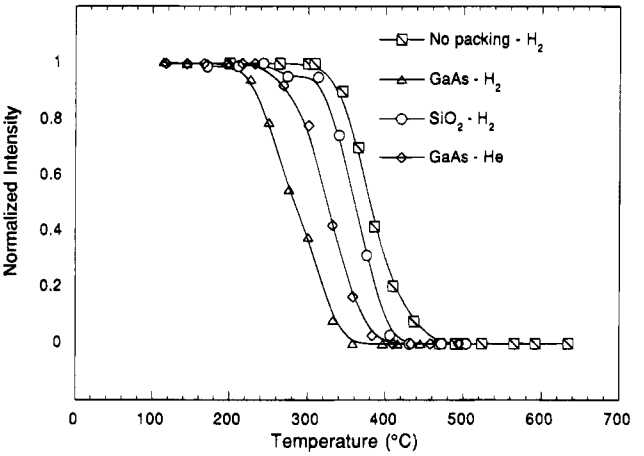

Figure 15. Decomposition of DMAAs in the presence of a high surface area of SiO_2 and GaAs.

The breaking of the C–N bond at elevated temperatures is a likely explanation for the observed nitrogen incorporation in AlGaAs.[6] Alternatively, the nitrogen incorporation may be attributed to strong interactions of the tris(dimethylamino) reagents with group III alkyls.[32] In any case, the onset of decomposition of the dimethylamine group marks the upper limit for gas-phase temperatures suitable for growth of high-quality III–V compound semiconductors with the new tris-(dimethylamino) reagents.

Surface Effects. The possible role of reactor surfaces in the decomposition reactions was explored by DMAAs by introducing large surface areas of SiO_2 and GaAs, as described in the Experimental Section. The degree of pyrolysis of DMAAs was affected by the presence of a high surface area of packing materials (see Figure 15). In the presence of a high surface area of SiO_2, the decomposition temperature is lowered less than 25 °C, and the product distribution remains similar to that observed for the "empty" cell. These observations suggest that the decomposition reactions observed in the original gas cell proceed through homogeneous pathways.

Heterogeneous reactions are clearly involved when the cell is packed with GaAs chips. Decomposition starts at 250 °C, about 100 °C lower than the results presented above for the empty gas cell. The first major reaction product to appear with increasing decomposition temperature is dimethylamine, followed by methylmethyleneimine about 50 °C above the initial decomposition temperature. The DMAAs pyrolysis behavior over a GaAs surface is in agreement with results of temperature-programmed desorption (TPD) studies of DMAAs on GaAs,[9] which show that the primary channel for DMAAs is surface reactions involving the generation of dimethylamine radicals.[9] The presence of H_2 again accelerates the decomposition relative to the He case by the gas-phase formation of $H^{\bullet}$, which subsequently attacks the parent molecule (cf. reactions 2 and 3). Methylmethyleneimine is most likely produced in gas-phase reactions (e.g., reaction 4), but some methylmethyleneimine could also result from a β-hydrogen transfer surface reaction pathway reported in TPD investigations.[9]

(32) Sateria, S.; Jensen, K. F., manuscript in preparation.

Conclusions

Pyrolysis studies of tris(dimethylamino)phosphine, -arsine, and -stibine precursors for OMCVD of InP, GaAs, InSb, and related compounds show that the reagents primarily decompose through homolysis of the central atom (P, A, Sb)–dimethylamine bond. The decomposition occurs at relatively lower temperatures than the trialkyl sources. Moreover, the corresponding group V species is formed without detectable side reactions to other organo group V reactions. These characteristics make the tris(dimethylamino) reagents suitable candidates for synthesis of III–V compound semiconductors, provided the gas-phase temperature above the growth surface is low enough to avoid decomposition of the dimethylaminyl radical and related species. The large number of lone-pair orbitals on the amino groups, as well as the central group V atom, however, raise the possibility of strong Lewis acid–base interactions leading to the formation of adducts with group III alkyls.[32] Such interactions could potentially result in reduced growth performance.

Acknowledgment. This work was supported by The National Science Foundation (DMR 9023162). The authors wish to thank Dr. David Bohling, Air Products and Chemicals, for donating the tris(dimethylamino) sources and for his interest in the work.

CM940411C